



**HAL**  
open science

## Test of GOCE EGG data for spacecraft positioning

Xiucong Sun, Pei Chen,, Yalong Han, Christophe Macabiau, Chao Han,

► **To cite this version:**

Xiucong Sun, Pei Chen,, Yalong Han, Christophe Macabiau, Chao Han,. Test of GOCE EGG data for spacecraft positioning. 5th International GOCE user workshop, European Space Agency (ESA), Nov 2014, Paris, France. hal-01159184

**HAL Id: hal-01159184**

**<https://enac.hal.science/hal-01159184>**

Submitted on 2 Jun 2015

**HAL** is a multi-disciplinary open access archive for the deposit and dissemination of scientific research documents, whether they are published or not. The documents may come from teaching and research institutions in France or abroad, or from public or private research centers.

L'archive ouverte pluridisciplinaire **HAL**, est destinée au dépôt et à la diffusion de documents scientifiques de niveau recherche, publiés ou non, émanant des établissements d'enseignement et de recherche français ou étrangers, des laboratoires publics ou privés.

# TEST OF GOCE EGG DATA FOR SPACECRAFT POSITIONING

Xiucong Sun<sup>(1)</sup>, Pei Chen<sup>(1)</sup>, Yalong Han<sup>(1)</sup>, Christophe Macabiau<sup>(2)</sup>, Chao Han<sup>(1)</sup>

<sup>(1)</sup> Beihang University, 37 Xueyuan Road, Beijing, 100191, China, Email: sunxiucong@gmail.com

<sup>(1)</sup> Beihang University, 37 Xueyuan Road, Beijing, 100191, China, Email: cjhien@gmail.com

<sup>(1)</sup> Beihang University, 37 Xueyuan Road, Beijing, 100191, China, Email: chittyhan@126.com

<sup>(2)</sup> ENAC, 7 Avenue Edouard BELIN, Toulouse, 31055, France, Email: macabiau@recherche.enac.fr

<sup>(1)</sup> Beihang University, 37 Xueyuan Road, Beijing, 100191, China, Email: hanchao@buaa.edu.cn

## ABSTRACT

Consisting of three pairs of accelerometers, the gradiometer is an ideal sensor for passive navigation. This paper proposes the use of gravity gradients for spacecraft positioning and the real-world GOCE EGG data are tested to investigate the feasibility. The basic observation equation is first formulated by considering white noise only, and a Least-Square position searching method is developed. The raw GGT measurements are preprocessed before the test in order to remove the low-frequency errors. By using a 120-degree EGM2008 gravity model as a reference map, position solutions with an accuracy of hundreds of meters are obtained. A further semi-simulation study shows that an accuracy of tens of meters could be achieved with a better gradiometer.

## 1. INTRODUCTION

The application of gravity gradiometry in navigation has been pursued for a long time. The gradiometer was first identified as an aid for the inertial navigation system (INS) in the 1960s with an intention to reduce errors from geodetic uncertainties [1]. Several integration methods were proposed and analysed around that time and laid the foundation for following studies [2-4]. In 1990, Affleck and Jircitano presented a passive gradiometer-aided INS based on gravity gradient map-matching technique [5]. The measured gravity gradient disturbances were compared with map values accessed by estimated positions, and the difference was processed by an optimal filter to provide corrections to position estimates, gradiometer error as well as map residual error. A combination of covariance and simulation analysis was carried out for low speed airborne and shipborne systems. Gleason continued the work and developed an efficient Fast Fourier Transformation algorithm to generate gridded gravity gradient maps [6]. Richeson presented discussions on the implementation of the map-matching method in his dissertation, and the navigation performance for a hypersonic cruise was investigated [7]. Simulation results showed that a hypothetical future grade gravity gradiometer instrument (GGI) with a noise level of 1 mE could provide GPS-like performance and bound the position error at decimetres. A comprehensive feasibility investigation was also conducted by Rogers in 2009,

and DeGregoria presented a thorough methodology study on aircraft navigation aiding in 2010 [8-9].

The common motivation in the studies of gravity gradient map-matching is that the gravity gradients contain useful position information and they are measured in a nonemanating way. Spoofing or jamming is impossible unless the local gravity field is changed. However, two obstacles concerning to ultra-low-noise gradiometers and accurate gravity gradient maps must be overcome in order to make this technology a reality, as stated in the study of Rogers [8]. The first instrument problem is easing due to the emerging superconducting technology as well as innovative researches in cold atom interferometry [7]. By contrast, the gravity gradient map construction faces a theoretical obstacle that the Earth mass density variability is unknown. A compromising method is to use global gravity models to compute gravity gradients. Terrain elevation data must also be included at low altitudes [6].

Things will be a little different when it comes to a low earth orbit (LEO) satellite. First, unlike vehicles at or near the Earth's surface, the spacecraft are not subject to large non-gravitational forces and thus follows a nearly free-fall motion. This ideal stabilization provides a good measurement platform for gradiometers. For example, the Electrostatic Gravity Gradiometer (EGG) onboard the ESA's GOCE satellite demonstrated an accuracy of  $0.01 \text{ E}/\sqrt{\text{Hz}}$  in the designed measurement bandwidth (MBW) when enhanced with a drag-free flight mode [10]. Second, since the gravity gradients attenuate proportional to distance cubed, some of the terrain contributions to the gravity field will be negligible at sufficiently high altitudes. Referring to analysis in [7], a satellite in a 300 km altitude orbit with a space-grade  $0.01 \text{ E}$  GGI noise level would only be affected by terrain effects greater than about 500 m tall. Thus a truncated spherical harmonic gravity model will be accurate enough for space users to generate gradient maps. Last but not least, high-precision attitude measurements can be easily obtained from star trackers for a spacecraft. The importance of the attitude information will be explained in the next section.

This paper investigates the feasibility of using gravity gradients as an observable for spacecraft navigation. Different from the filter updating map-matching technique for inertial navigation aiding [5, 7-9], the method proposed in this paper aims to resolve position

directly from epoch-wise gravity gradient measurements. An assumption is made that there are no measurement bias or information missing and only the white noise disturbance needs to be considered. It is a practical assumption in that any bias or missing information can be compensated or recovered by estimation and calibration techniques. To evaluate the observability and to test the positioning performance, the GOCE EGG data are used. The GOCE satellite was the first-ever satellite to carry a gradiometer in space, and large amounts of gravity gradients were measured from an unprecedented low altitude of about 260 km [11]. Two high performance GPS receivers and three advanced star trackers were also mounted on the satellite. The GPS measurements have already been processed by ESA to generate precise orbit solutions (PSO) with an accuracy of about 2 cm [12]. The known orbits are used to validate the accuracy of position estimates obtained from gravity gradient observations.

The remainder of this paper is organised as follows. Section 2 introduces the mathematical model of gravity gradients as functions of position, and the observation equation in the gradiometer reference frame (GRF) is formulated. Section 3 presents an Eigen-Decomposition algorithm for initial position determination followed by a Least-Square estimator to iterate positions. Covariance analysis equation is also given to estimate the position errors. Section 4 describes the error characteristics of GOCE EGG measurements as well as the preprocessing work needed before the test. Section 5 summarized the test results and Section 6 presents the conclusions.

## 2. GRAVITY GRADIENTS AS FUNCTIONS OF POSITION

The gravity gradients (“gravitational gradients” more precisely) are the spatial derivatives of the gravitational acceleration, and are expressed as a second-order tensor in mathematics:

$$\mathbf{V} = \frac{\partial \mathbf{g}}{\partial \mathbf{r}^T} = \begin{bmatrix} \frac{\partial g_x}{\partial x} & \frac{\partial g_x}{\partial y} & \frac{\partial g_x}{\partial z} \\ \frac{\partial g_y}{\partial x} & \frac{\partial g_y}{\partial y} & \frac{\partial g_y}{\partial z} \\ \frac{\partial g_z}{\partial x} & \frac{\partial g_z}{\partial y} & \frac{\partial g_z}{\partial z} \end{bmatrix} \quad (1)$$

where  $\mathbf{g}$  is the gravitational acceleration,  $\mathbf{r}$  is the position vector, and  $(g_x, g_y, g_z)$  and  $(x, y, z)$  are the vector components of  $\mathbf{g}$  and  $\mathbf{r}$  with respect to a specific cartesian coordinate system.

The gravity gradient tensor (GGT) is unique for position relative to the Earth (but not exactly for a central gravitational force field). The Earth-Centered Earth-Fixed (ECEF) coordinate system is a natural reference frame for GGT representation and a spherical harmonic model is provided in geodesy to express the gravity

gradients as functions of position:

$$V_{ij}^E = \frac{GM}{R} \sum_{n=0}^{\infty} \sum_{m=0}^n \left( C_{nm} \frac{\partial^2 A_{nm}}{\partial i \partial j} + S_{nm} \frac{\partial^2 B_{nm}}{\partial i \partial j} \right) \quad (2)$$

where  $V_{ij}^E$  are components of GGT in the ECEF frame,  $i$  and  $j$  take values from  $x$ ,  $y$  and  $z$ ,  $G$  is the gravitational constant,  $M$  is the mass of the Earth,  $R$  is the radius of the Earth,  $n$  and  $m$  are degree and order, and  $C_{nm}$  and  $S_{nm}$  are spherical harmonic coefficients.  $A_{nm}$  and  $B_{nm}$  are functions of position and defined as:

$$\begin{aligned} A_{nm} &= \left( \frac{R}{r} \right)^{n+1} P_{nm}(\sin \phi) \cos(m\lambda) \\ B_{nm} &= \left( \frac{R}{r} \right)^{n+1} P_{nm}(\sin \phi) \sin(m\lambda) \end{aligned} \quad (3)$$

where  $r$ ,  $\phi$  and  $\lambda$  are the geocentric coordinates of the observation position in ECEF, and  $P_{nm}$  is the Legendre function.

A full-tensor gradiometer cannot sense  $V_{ij}^E$  directly, and it only measures GGT in its reference frame, which is defined by the three orthogonal arms of the six accelerometers. Let  $\mathbf{V}^E$  and  $\mathbf{V}^G$  denote GGTs in the ECEF and GRF frame respectively.  $\mathbf{V}^E$  can be transformed to  $\mathbf{V}^G$  by the following equation:

$$\mathbf{V}^G = \mathbf{R}_E^G \mathbf{V}^E (\mathbf{R}_E^G)^T \quad (4)$$

where  $\mathbf{R}_E^G$  is the rotation matrix from ECEF to GRF.

As GGT is symmetric, the GOCE gradiometer outputs 6 components of  $\mathbf{V}^G$ . By introducing the column vectors:

$$\begin{aligned} \mathbf{V}_l^G &= [V_{xx}^G \ V_{yy}^G \ V_{zz}^G \ V_{xy}^G \ V_{xz}^G \ V_{yz}^G]^T \\ \mathbf{V}_l^E &= [V_{xx}^E \ V_{yy}^E \ V_{zz}^E \ V_{xy}^E \ V_{xz}^E \ V_{yz}^E]^T \end{aligned} \quad (5)$$

an observation equation is formulated as follows:

$$\begin{aligned} \mathbf{Z} &= \mathbf{V}_l^G + \mathbf{v} \\ &= \mathbf{T}_E^G \mathbf{V}_l^E + \mathbf{v} \end{aligned} \quad (6)$$

where  $\mathbf{Z}$  is the column set of observations, and  $\mathbf{v}$  is the measurement noise.  $\mathbf{T}_E^G$  is a  $6 \times 6$  matrix composed of elements from the rotation matrix  $\mathbf{R}_E^G$ :

$$\mathbf{T}_E^G = \begin{bmatrix} c_{11}^2 & c_{12}^2 & c_{13}^2 & 2c_{11}c_{12} & 2c_{11}c_{13} & 2c_{12}c_{13} \\ c_{21}^2 & c_{22}^2 & c_{23}^2 & 2c_{21}c_{22} & 2c_{21}c_{23} & 2c_{22}c_{23} \\ c_{31}^2 & c_{32}^2 & c_{33}^2 & 2c_{31}c_{32} & 2c_{31}c_{33} & 2c_{32}c_{33} \\ c_{11}c_{21} & c_{12}c_{22} & c_{13}c_{23} & c_{12}c_{21} + c_{11}c_{22} & c_{13}c_{21} + c_{11}c_{23} & c_{13}c_{22} + c_{12}c_{23} \\ c_{11}c_{31} & c_{12}c_{32} & c_{13}c_{33} & c_{12}c_{31} + c_{11}c_{32} & c_{13}c_{31} + c_{11}c_{33} & c_{13}c_{32} + c_{12}c_{33} \\ c_{21}c_{31} & c_{22}c_{32} & c_{23}c_{33} & c_{22}c_{31} + c_{21}c_{32} & c_{23}c_{31} + c_{21}c_{33} & c_{23}c_{32} + c_{22}c_{33} \end{bmatrix} \quad (7)$$

where  $c_{ij}$  is the  $i^{\text{th}}$  row and  $j^{\text{th}}$  column of  $\mathbf{R}_E^G$ . A similar expression is also found in [7].

The observations contains both position and attitude information. Recalling Eq. 2,  $\mathbf{V}_I^E$  is a function of position only. Rotation matrix  $\mathbf{R}_E^G$  is in reality a production of two matrices:

$$\mathbf{R}_E^G = \mathbf{R}_I^G \mathbf{R}_E^I \quad (8)$$

where  $\mathbf{R}_E^I$  is the rotation matrix from ECEF to the inertial frame, and  $\mathbf{R}_I^G$  is the rotation matrix from the inertial frame to GRF. Earth Orientation Parameters (EOP) as well as gradiometer attitudes are required to compute these matrices. Star trackers nowadays can provide attitude measurements with an accuracy of a few arcseconds [13], corresponding to a rotation precision of  $5 \times 10^{-6}$ . The transformation error of gravity gradients due to attitude error is around 0.01 E. The precision of rotation matrix  $\mathbf{R}_E^I$  is even better. The latest IERS report shows an accuracy of better than  $1 \times 10^{-8}$  has been achieved for the Earth rotation matrix [14]. The GGT transformation error caused by EOP error is smaller than 0.1 mE. The transformation errors are all incorporated into the measurement noise, which will be discussed in the next section. Thus, with EOP data and high precision attitude measurements provided, Eq. 6 becomes an observation for position only.

### 3. POSITION ESTIMATION AND COVARIANCE ANALYSIS

This section investigates the use of a nonlinear Least-Square estimator to resolve position. An initial value must be provided at first. Since GGT is a symmetric matrix, Eigen-Decomposition can be performed. In a central gravitational force field,  $\mathbf{V}^E$  has a simple expression:

$$\mathbf{V}^E = \frac{GM}{r^3} \begin{bmatrix} -1 + \frac{3x^2}{r^2} & \frac{3xy}{r^2} & \frac{3xz}{r^2} \\ \frac{3xy}{r^2} & -1 + \frac{3y^2}{r^2} & \frac{3yz}{r^2} \\ \frac{3xz}{r^2} & \frac{3yz}{r^2} & -1 + \frac{3z^2}{r^2} \end{bmatrix} \quad (9)$$

The Eigen-Decomposition of  $\mathbf{V}^E$  is:

$$\mathbf{V}^E = \mathbf{\Phi} \mathbf{\Gamma} \mathbf{\Phi}^T \quad (10)$$

where:

$$\mathbf{\Gamma} = \frac{GM}{r^3} \begin{bmatrix} -1 & 0 & 0 \\ 0 & -1 & 0 \\ 0 & 0 & 2 \end{bmatrix} \quad (11)$$

$$\mathbf{\Phi} = \begin{bmatrix} -\sin \lambda & -\sin \phi \cos \lambda & \cos \phi \cos \lambda \\ \cos \lambda & -\sin \phi \sin \lambda & \cos \phi \sin \lambda \\ 0 & \cos \phi & \sin \phi \end{bmatrix}$$

The diagonal elements of  $\mathbf{\Gamma}$  are eigenvalues, and the three column vectors in  $\mathbf{\Phi}$  are the corresponding eigenvectors. From Eq. 11, the eigenvalues are function

of  $r$  only, and the eigenvectors are functions of  $\phi$  and  $\lambda$ . Let  $\xi$  denote the maximum eigenvalue and  $\boldsymbol{\eta}$  denote the corresponding eigenvector, i.e.:

$$\xi = 2GM/r^3 \quad (12)$$

$$\boldsymbol{\eta} = [\cos \phi \cos \lambda \quad \cos \phi \sin \lambda \quad \sin \phi]^T$$

Then an initial position can be obtained by  $\xi$  and  $\boldsymbol{\eta}$ :

$$\hat{\mathbf{r}}_0 = \left( \frac{2GM}{\xi} \right)^{1/3} \boldsymbol{\eta} \quad (13)$$

It must be noted that a sign ambiguity exists for  $\boldsymbol{\eta}$ . This positive/negative problem is due to the centrosymmetric property of the central gravitational force field. The problem will be addressed later.

With the initial values ( $\pm$ ) provided by Eq. 13, an iterative nonlinear estimator using a high-degree gravity model will be applied to search the exact positions at which the computed GGTs match the observations. In this paper, a 120-degree EGM2008 gravity model is used as a reference map to compute gravity gradients.

The error sources of the measurement noise  $\mathbf{v}$  in Eq. 6 include not only the gradiometer noise but also the GGT transformation uncertainties as well as the map residual error. In this paper the components of the measurement noise  $\mathbf{v}$  are assumed to be independent and zero-mean Gaussian random variables. Let  $\mathbf{Q}$  denote the noise covariance matrix. The Least-Square iteration is given as follows:

$$\hat{\mathbf{r}}_{k+1} = \hat{\mathbf{r}}_k + (\mathbf{H}_k^T \mathbf{Q}^{-1} \mathbf{H}_k)^{-1} \mathbf{H}_k^T \mathbf{Q}^{-1} (\mathbf{Z} - \mathbf{V}_I^G(\hat{\mathbf{r}}_k)) \quad (14)$$

where  $\mathbf{H}_k$  is the Jacobian matrix of  $\mathbf{V}_I^G$  with respect to  $\mathbf{r}$  at the  $k^{\text{th}}$  estimated position:

$$\mathbf{H}_k = \left. \frac{\partial \mathbf{V}_I^G}{\partial \mathbf{r}} \right|_{\mathbf{r}=\hat{\mathbf{r}}_k} = \mathbf{T}_E^G \left. \frac{\partial \mathbf{V}_I^E}{\partial \mathbf{r}} \right|_{\mathbf{r}=\hat{\mathbf{r}}_k} \quad (15)$$

The computation of  $\mathbf{H}_k$  involves the partial derivatives of  $\mathbf{V}_I^E$  with respect to position:

$$\frac{\partial V_{ij}^E}{\partial p} = \frac{GM}{R} \sum_{n=0}^{\infty} \sum_{m=0}^n \left( C_{nm} \frac{\partial^3 A_{nm}}{\partial i \partial j \partial p} + S_{nm} \frac{\partial^3 B_{nm}}{\partial i \partial j \partial p} \right) \quad (16)$$

where  $i, j$  and  $p$  take values from  $x, y$  and  $z$ . A low-degree gravity model could be used to compute these partial derivatives. In this paper, the maximum degree and order for this computation is 2 and 0.

The covariance of the position estimates can be determined via the covariance analysis:

$$\text{Cov}(\hat{\mathbf{r}}_{k+1}) \equiv E \left[ (\hat{\mathbf{r}}_{k+1} - \mathbf{r})(\hat{\mathbf{r}}_{k+1} - \mathbf{r})^T \right] \quad (17)$$

$$= (\mathbf{H}_{k+1}^T \mathbf{Q}^{-1} \mathbf{H}_{k+1})^{-1}$$

Each component's standard deviation (SD) can be used as a measure of estimated spacecraft position accuracy.

Recall the sign ambiguity problem. A statistical tool can be used. The observation residuals are expected to be normally distributed with zero mean and variance  $\mathbf{Q}$ :

$$\begin{aligned} E[\mathbf{Z} - \mathbf{V}^G(\hat{\mathbf{r}}_{k+1})] &= \mathbf{0} \\ E[(\mathbf{Z} - \mathbf{V}^G(\hat{\mathbf{r}}_{k+1}))(\mathbf{Z} - \mathbf{V}^G(\hat{\mathbf{r}}_{k+1}))^T] &= \mathbf{Q} \end{aligned} \quad (18)$$

Any mismatches in the statistical means or the standard deviations will be applied to identify the incorrect solutions iterated from the initial values with wrong signs.

#### 4. PREPROCESSING OF GOCE EGG DATA FOR POSITIONING TEST

The measurement data used in the test are the EGG\_GGT\_1i data block from the EGG\_NOM\_1b product. These data contain in-flight calibrated gravity gradients without temporal correction (the tidal and nontidal effects) or external calibration, and can be viewed as raw measurements. Actually, the temporal terms of gravity gradients are negligible compared with the measurement error, and the in-flight calibrated parameters (scale factors) are accurate enough [15].

In the observation equation (Eq. 6 in Section 2) the measurement error is modelled as low-level white noise. The GOCE EGG sensor, however, only minimizes GGT error in MBW between 5 mHz and 0.1 Hz. Below MBW the error power spectral density (PSD) has a  $1/f$  behaviour. And the error dominates the signal below the orbit revolution frequency [15]. This kind of error cannot be handled by the position estimation technique directly. Thus the  $1/f$  error must be removed before using the GGT measurements for position fix.

A Fourier series model is adopted in this paper to model the  $1/f$  error in each gravity gradient observation component:

$$\Delta = \alpha + \beta \cdot t + \sum_{k=1}^K [a_k \cos 2\pi k f_0 t + b_k \sin 2\pi k f_0 t] \quad (19)$$

where  $\Delta$  is the  $1/f$  error,  $\alpha$  is bias,  $\beta$  is trend,  $f_0$  is the base frequency and equals the orbit revolution frequency, and  $a_k$  and  $b_k$  are Fourier coefficients. The maximum order of the sinusoid terms,  $K$ , is chosen to satisfy that  $Kf_0 = 5$  mHz. Thus, the model can represent most of the error below MBW in one orbit period.

To resolve the  $2+2K$  unknown coefficients  $\alpha$ ,  $\beta$ ,  $a_k$ , and  $b_k$ , precise model reference values must be computed. A 300-degree EGM2008 gravity model are selected, and precise position and attitude information from SST\_PSO\_2 and EGG\_IAQ\_1i are also utilized. The coefficients are resolved by a linear Least-Square estimator every orbit period and then subtracted from the GGT measurements.

An alternative is to treat the  $1/f$  error as a state variable and to estimate it along with position estimation. This is the truth for the navigation process. However the

objective of the test in this paper is to investigate the observability of GGT for positioning. The error preprocessing is reasonable.

#### 5. TEST RESULTS

The data collected on 8 September 2013 covering 16 orbit periods are tested. With a sampling rate of 1 Hz and a mean orbit period of 5339 s, the total number of epochs is 85424. The  $1/f$  error is first calculated and removed from the gravity gradients by the preprocessing techniques described in Section 4. The accuracy of the recovered gravity gradients is shown in Fig. 1.

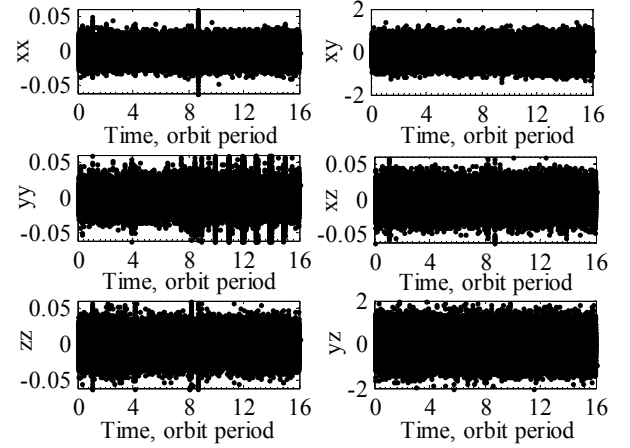


Figure 1. The Error of the Recovered Gravity Gradients (unit, E)

From Fig. 1, large errors exist at some epochs because the outlier detection is not applied. The mean errors of the 6 components are all near zero, and the standard deviations (SDs) are 0.0097 E, 0.012 E, 0.013 E, 0.33 E, 0.013 E and 0.49 E respectively, which indicates that only the low-level flat noise is left. The noise covariance matrix  $\mathbf{Q}$  is set to:

$$\mathbf{Q} = \begin{bmatrix} 0.011^2 & & & & & \\ & 0.011^2 & & & & \\ & & 0.011^2 & & & \\ & & & 0.35^2 & & \\ & & & & 0.011^2 & \\ & & & & & 0.50^2 \end{bmatrix} E^2 \quad (20)$$

The Eigen-Decomposition method produces two sets of initial positions. Fig. 2 plots the errors of the correct set of initial positions in the ECEF frame, with a mean three dimensional (3D) error of  $1.2 \times 10^4$  m.

With these initial values, the nonlinear Least-Square estimator performs iterations according to Eq. 14 until the update is below 1 m. The search process usually ends after 4 or 5 iterations. Fig. 3 gives the errors of the final searched positions (correct ones) in ECEF as well as the standard deviations (red lines) obtained from covariance analysis. It is seen that the standard

deviations can well describe the actual position errors.

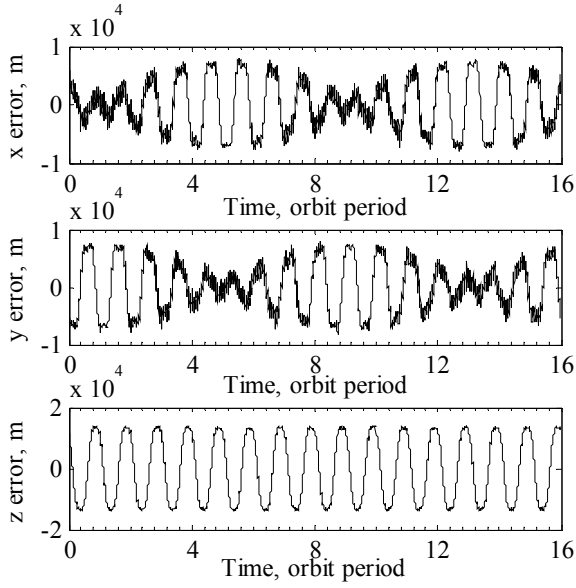


Figure 2. Errors of the Three Components of Initial Positions (correct ones) in the ECEF Frame

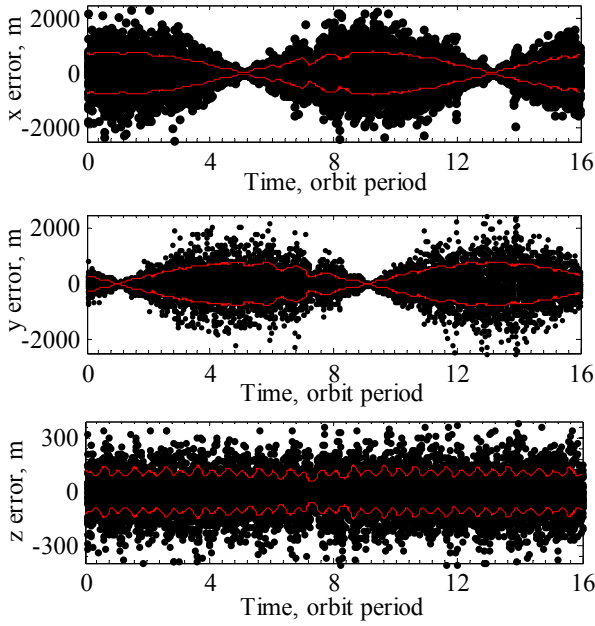


Figure 3. The Errors (black points) and Standard Deviations ( $\pm$ , red lines) of the Final Searched Positions (correct ones)

From Fig. 3, the errors of the  $x$  and  $y$  components show sinusoidal changes with the same period of 12 hours. That is because the relative orientation of the GRF frame with respect to the ECEF frame repeats every 12 hours (not considering the positive/negative direction) and the two noisy observation components of  $V_{xy}^G$  and  $V_{yz}^G$  are closely related to the  $x$  and  $y$  components (seen

from Eq. 9). The maximum and minimum standard deviations of the  $x$  and  $y$  components are 800 m and 8 m respectively, and the standard deviation of the  $z$  component is nearly constant with mean value of 109 m. The mean 3D position error is 620 m.

The incorrect position solutions are identified from the observation residuals. Tab. 1 lists the statistical means and standard deviations of the observation residuals. It is shown that the residuals corresponding to the correct solutions satisfy the expectation given in Eq. 18, whereas some mismatches exist in standard deviations (in bold) for the incorrect solutions.

Table 1. Statistical Means and Standard Deviations of the Observation Residuals

Component	Mean $\pm$ Standard Deviation (E)	
	Correct solutions	Incorrect solutions
$xx$	$8.9 \times 10^{-5} \pm 0.010$	$-1.6 \times 10^{-3} \pm \mathbf{0.11}$
$yy$	$-2.3 \times 10^{-4} \pm 0.015$	$1.4 \times 10^{-3} \pm \mathbf{0.11}$
$zz$	$-7.5 \times 10^{-5} \pm 7.6 \times 10^{-3}$	$-7.5 \times 10^{-5} \pm 7.6 \times 10^{-3}$
$xy$	$2.8 \times 10^{-3} \pm 0.33$	$2.1 \times 10^{-3} \pm 0.35$
$xz$	$1.2 \times 10^{-6} \pm 8.9 \times 10^{-5}$	$-4.9 \times 10^{-5} \pm 9.4 \times 10^{-4}$
$yz$	$-6.4 \times 10^{-3} \pm 0.24$	$\mathbf{-0.11 \pm 2.2}$

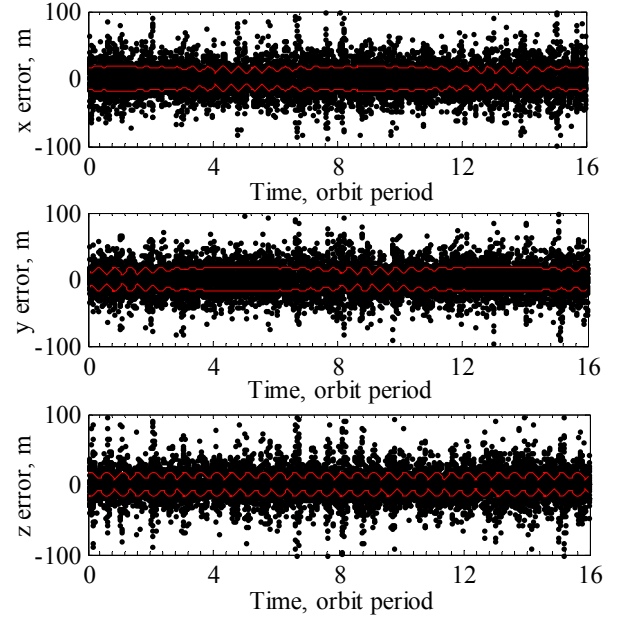


Figure 4. The Errors (black points) and Standard Deviations ( $\pm$ , redlines) of Position Estimates (correct ones) for the Semi-Simulation Case

To assess the improvement in position accuracy by using a more accurate gradiometer, a semi-simulation test is carried out. The noisy observation components of  $V_{xy}^G$  and  $V_{yz}^G$  are replaced with simulated measurements which have the same noise level as the other 4

components, i.e., 0.11 E. As illustrated in Fig. 4, the mean standard deviations of three position components are reduced to 15.4 m, 15.4 m and 13.0 m respectively, and the mean 3D position error is reduced to 33.4 m.

## 6. CONCLUSIONS

This research presents a promising use of gravity gradiometry for space navigation. The GOCE EGG data are tested to investigate the feasibility of spacecraft positioning from gravity gradients. The developed Least-Square approach makes use of high-degree spherical gravity models to search positions at which the computed gravity gradients match the observations. Eigen-Decomposition of GGT provides initial values but produces sign ambiguity at the same time. Statistical analysis of observation residuals is suggested in this paper to kick out the incorrect position solutions. The GOCE real data show a limited ability to fix positions due to the two noisy observation components. However, tens of meters of accuracy is achieved in the semi-simulation analysis using a better gradiometer. With the development of gradiometer technology as well as gravity models, it is foreseen that improvements in the navigation performance will be realized one day.

## ACKNOWLEDGEMENT

The authors acknowledge the European Space Agency for the provision of the GOCE data.

## REFERENCES

1. Britting, K. R., Madden, S. J. & Hildebrant, R. A. (1972). The Impact of Gradiometer Techniques on the Performance of Inertial Navigation Systems. In *AIAA Guidance and Control Conference*, AIAA 72-850, Stanford, California, US.
2. Grubin, C. (1975). Accuracy Improvement in a Gravity Gradiometer-Aided Cruise Inertial Navigator Subjected to Deflections of the Vertical. In *AIAA Guidance and Control Conference*, AIAA 75-1090, Boston, US.
3. Heller, W. G. & Jordan, S. K. (1975). Mechanization and Error Equations for Two New Gradiometer-Aided Inertial Navigation System Configurations. In *AIAA Guidance and Control Conference*, AIAA 75-1091, Boston, US.
4. Metzger, E. H. & Jircitano, A. (1975). Inertial Navigation Performance Improvement Using Gravity Gradient Matching Techniques. In *AIAA Guidance and Control Conference*, AIAA 75-1092, Boston, US.
5. Affleck, C. A. & Jircitano, A. (1990). Passive Gravity Gradiometer Navigation System. In *IEEE PLANS, Position Location and Navigation Symposium*, Las Vegas, US, pp60-66.
6. Gleason, D. M. (1995). Passive Airborne Navigation and Terrain Avoidance Using Gravity Gradiometry. *J Guid Control Dynam.* **18**(6), 1450-1458.
7. Richeson, J. A. (2008). Gravity Gradiometer Aided Inertial Navigation within Non-GNSS Environments. Ph. D. Dissertation, University of Maryland, US.
8. Rogers, M. M. (2009). An Investigation into the Feasibility of Using a Modern Gravity Gradient Instrument for Passive Aircraft Navigation and Terrain Avoidance. Master's Thesis, Air Force Institute of Technology, US.
9. DeGregoria, A. (2010). Gravity Gradiometry and Map Matching: an Aid to Aircraft Inertial Navigation Systems. Master's Thesis, Air Force Institute of Technology, US.
10. Bouman, J., Fiorot, S., Fuchs, M., Gruber, T., Schrama, E., Tscherning, C., Veicherts, M. & Visser, P. (2011). GOCE Gravitational Gradients along the Orbit. *J Geod.* **85**(11), 791-805.
11. Floberghagen, R., Fehring, M., Lamarre, D., Muzi, D., Frommknecht, B., Steiger, C., Piñeiro, J. & Da Costa, A. (2011). Mission Design, Operation and Exploitation of the Gravity Field and Steady-State Ocean Circulation Explorer Mission. *J Geod.* **85**(11), 749-758.
12. Bock, H., Jäggi, A., Meyer, U., Visser, P., van den Ijssel, J., van Helleputte, T., Heinze, M. & Hugentobler, U. (2011). GPS-derived Orbits for the GOCE Satellite. *J Geod.* **85**(11), 807-818.
13. Liebe, C. C. (2002). Accuracy Performance of Star Trackers—A Tutorial. *IEEE T Aero Elec Sys.* **38**(2), 587-599.
14. Petit, G. & Luzum, B. (2010). *IERS Conventions (2010)*. IERS Technical Note 36, Verlag des Bundesamts für Kartographie und Geodäsie.
15. Bouman, J., Rispens, S., Gruber, T., Koop, R., Schrama, E., Visser, P., Tscherning, C. C. & Veicherts, M. (2009). Preprocessing of Gravity Gradients at the GOCE High-Level Processing Facility. *J Geod.* **83**(7), 659-678.